ARTICLE

Transforming activities of the *NUP98-KMT2A* fusion gene associated with myelodysplasia and acute myeloid leukemia

James N. Fisher,[1,2*] Angeliki Thanasopoulou,[1,2*] Sabine Juge,[1,2] Alexandar Tzankov,[3] Frederik O. Bagger,[1,2] Max A. Mendez,[1,2] Antoine H.F.M. Peters[4,5] and Juerg Schwaller[1,2]

[1]University Children's Hospital Basel (UKBB); [2]Department of Biomedicine, University of Basel; [3]Institute for Pathology, University of Basel; [4]Faculty of Sciences, University of Basel and [5]Friedrich Miescher Institute for Biomedical Research, Basel, Switzerland

**JNF and ATh contributed equally as co-first authors.*

Ferrata Storti Foundation

Haematologica 2020
Volume 105(7):1857-1867

ABSTRACT

Inv(11)(p15q23), found in myelodysplastic syndromes and acute myeloid leukemia, leads to expression of a fusion protein consisting of the N-terminal of nucleoporin 98 (NUP98) and the majority of the lysine methyltransferase 2A (KMT2A). To explore the transforming potential of this fusion we established inducible iNUP98-KMT2A transgenic mice. After a median latency of 80 weeks, over 90% of these mice developed signs of disease, with anemia and reduced bone marrow cellularity, increased white blood cell numbers, extramedullary hematopoiesis, and multilineage dysplasia. Additionally, induction of *iNUP98-KMT2A* led to elevated lineage marker-negative Sca-1$^+$ c-Kit$^+$ cell numbers in the bone marrow, which outcompeted wildtype cells in repopulation assays. Six *iNUP98-KMT2A* mice developed transplantable acute myeloid leukemia with leukemic blasts infiltrating multiple organs. Notably, as reported for patients, iNUP98-KMT2A leukemic blasts did not express increased levels of the *HoxA-B-C* gene cluster, and in contrast to KMT2A-AF9 leukemic cells, the cells were resistant to pharmacological targeting of menin and BET family proteins by MI-2-2 or JQ1, respectively. Expression of *iNUP98-KMT2A* in mouse embryonic fibroblasts led to an accumulation of cells in G1 phase, and abrogated replicative senescence. In bone marrow-derived hematopoietic progenitors, iNUP98-KMT2A expression similarly resulted in increased cell numbers in the G1 phase of the cell cycle, with aberrant gene expression of *Sirt1*, *Tert*, *Rbl2*, *Twist1*, *Vim*, and *Prkcd*, mimicking that seen in mouse embryonic fibroblasts. In summary, we demonstrate that *iNUP98-KMT2A* has *in vivo* transforming activity and interferes with cell cycle progression rather than primarily blocking differentiation.

Introduction

The gene encoding the 98 kDa nuclear pore protein (NUP98) is recurrently involved in chromosomal translocations associated with various hematologic malignancies. Most of these translocations result in the expression of fusion genes comprising the N-terminal phenylalanine-glycine (FG)-repeats of *NUP98* fused to a large group of different partners of which the homeobox family of transcription factors (such as *HOXA9* or *HOXD13*) or non-homeobox epigenetic regulators are a part.[1,2] Like *NUP98*, the lysine methyltransferase *KMT2A*, also referred to as "mixed lineage leukemia" (*MLL*) gene, encoding for a SET-domain histone H3K4 methyltransferase is a recurrent target of leukemia-associated chromosomal rearrangements. These generally lead to expression of fusion transcripts that contain the amino-terminal moiety of *KMT2A* fused to different partners, of which *AF4*, *AF9*, *ENL* and *AF10* are among the most prevalent of the currently more than 70 known.[3,4] Several *KMT2A* fusions have been shown to be hematopoietic oncogenes, which phenocopy the disease *in vivo* when expressed in murine bone mar-

Correspondence:

JUERG SCHWALLER
j.schwaller@unibas.ch

Received: March 1, 2019.

Accepted: September 24, 2019.

Pre-published: September 26, 2019.

doi:10.3324/haematol.2019.219188

Check the online version for the most updated information on this article, online supplements, and information on authorship & disclosures: www.haematologica.org/content/105/7/1857

row (BM).[3-6] In cases in which these fusions do not contain the KMT2A-SET (suppressor of variegation 3–9, enhancer of zeste, and trithorax) domain, they acquire H3K79 or H4R3 histone methyltransferase- or acetyltransferase activity through interactions with several co-factors.[5,6] The interaction between chromatin and KMT2A fusions, mediated by the N-terminal menin- and the LEDGF (lens epithelium-derived growth factor) binding domain, has been shown to be crucial for maintenance of the leukemic phenotype.[7-10] Exploration of the KMT2A-menin-LEDGF interaction triad has led to the development of a series of promising small molecules with potent antileukemic activity.[11,12] More recent studies have proposed physical interactions between NUP98, and NUP98 fusion proteins, with KMT2A and non-specific lethal histone-modifying protein complexes. Parallel genetic studies using mouse models suggested that NUP98-fusion gene driven leukemogenesis might be dependent on KMT2A function.[13-15]

Inv(11)(p15q23) has been reported as the sole chromosomal abnormality in patients with several hematologic malignancies including myelodysplastic syndromes (MDS) and acute myeloid leukemia (AML);[16-20] however, to date NUP98-KMT2A fusion expression has only been reported in two patients with AML.[19] Using fluorescent *in situ* hybridization and reverse transcription quantitative polymerase chain reaction (PCR), Kaltenbach *et al.* found that inv(11)(p15q23) leads to fusion of the *NUP98-FG*-repeats to almost the entire *KMT2A* open reading frame (ORF).[19] In this case, exon 1 encoding for the N-terminal menin-LEDGF interaction domain is lost. In contrast to other KMT2A- or NUP98-fusion associated diseases, NUP98-KMT2A$^+$ leukemic blasts did not express known KMT2A targets such as the *HOXA*-gene cluster (*HOXA5*, *HOXA7*, *HOXA9*, or *HOXA10*) suggesting alternative mechanisms of transformation. As the size of the *NUP98-KMT2A* fusion ORF (>12 kb) limits the ability to test its transforming activity by retroviral expression in BM cells, we generated an inducible transgenic mouse model. We found that *iNUP98-KMT2A* expression led to a symptomatic[21] hematologic disease mimicking human MDS or AML that, as in patients, was not associated with elevated expression of the *Hox-A-B-C* gene cluster.[19] Thus, our work formally proves that a fusion, in which the N-terminus of *KMT2A* is replaced by the FG-repeats of *NUP98*, is a leukemogenic oncogene.

Methods

Primary induction of iNUP98-KMT2A expression

Adult transgenic mice were provided with doxycycline-impregnated chow pellets (400 ppm Doxycycline Diet, Harlan-Teklad) *ad libitum* from 6-8 weeks of age until analysis. All experiments were conducted in compliance with Swiss animal welfare laws and were approved by the Swiss Cantonal Veterinary Office of Basel Stadt.

Flow cytometry, colony-forming assays and cell culture

Total BM cells were isolated from wildtype (WT) C57BL/6 and *iNUP98-KMT2A* mice and processed with the Direct Lineage Cell Depletion kit (Miltenyi Biotec, Bergisch Gladbach, Germany). For immunophenotypic analysis, cells were incubated with antibodies recognizing the mouse lineage markers: CD11b (Mac-1), Ly-6G (Gr-1), CD117 (c-Kit), FcγRII/III, Ter119, CD71, B220, CD3, and CD34. For lineage marker-negative Sca-1$^+$ c-Kit$^+$ (LSK) characterization, lineage marker negative (Lin$^-$) BM cells were stained with Ly-6A/E (Sca-1), c-Kit, CD150 (SLAM1) and CD48, as well as CD45.1 and CD45.2 antibodies.

For proliferation experiments, 1x10^5 Lin$^-$ BM cells were cultured in liquid media containing murine stem cell factor (100 ng/mL), murine interleukin 3 (6 ng/mL), human interleukin 6 (10 ng/mL) and doxycycline (1 μg/mL). For colony-forming assays, 5x10^3 Lin$^-$ cells were plated in 2 mL of methylcellulose (MethoCult M3434, StemCell Technologies, Vancouver, Canada) and counted after 8-10 days. For cell cycle analysis, cells were fixed for 16 h at 4°C in a 4% paraformaldehyde solution (Thermo Scientific, Monza, Italy) then stained with Hoechst 33342 (Invitrogen, Waltham, USA) and pyronin Y (Sigma, St. Louis, USA) for 40 min at room temperature, flowed for 15 min on ice, before washing in FACS buffer and analysis. For *in vitro* experiments, unless indicated otherwise, doxycycline was used at a concentration of 1 μg/mL.

PO-PRO-1 and 7-aminoactinomycin D staining of apoptotic cells

Apoptotic cells were quantified using the PO-PRO-1 and 7-aminoactinomycin D staining kit (Invitrogen, Waltham, USA) in accordance with the kit protocol.

Expression analysis of senescence-related genes in *iNUP98-KMT2A* mouse embryonic fibroblasts

Mouse embryonic fibroblasts (MEF) were generated by isolation of E14.5 embryos from *iNUP98-KMT2A* mice and the genotype was checked by PCR. To investigate senescence, WT and iNUP98-KMT2A MEF were grown in Dulbecco modified Eagle medium with doxycycline and serially passaged into 100 mm plates when 90% confluence was reached. β-Galactosidase staining was performed using the Senescence β-Galactosidase Staining kit (Cell Signaling, Leiden, the Netherlands) when WT MEF started showing signs of senescence. RNA was extracted from MEF cell pellets at early and late passages and senescence-related gene expression was analyzed by quantitative real-time PCR using a commercially available kit (RT2 Profiler PCR Array, QIAGEN AG, Hombrechtikon, Switzerland) (*Online Supplementary Table S2*) as well as by manual quantitative PCR using specific primers. Gene expression levels on the RT^2 Profiler PCR Array were normalized to an internal panel of housekeeping genes, whereas individual quantitative PCR data were normalized to *Gapdh*.

Exposure of leukemic blasts to menin and BET inhibitors

iNUP98-KMT2A and KMT2A-AF9 leukemic blasts were isolated and treated for 48 h *in vitro* with 0-500 nM of the BRD4 inhibitor JQ1/vehicle (dimethylsulfoxide, DMSO) or 0-12 μM of the menin-interaction inhibitor MI-2-2/vehicle (DMSO). Cell cycle analysis was performed at the 48 h time-point after staining with Hoechst 33342 and pyronin Y as described above.

Results

Establishing *iNUP98-KMT2A* transgenic mice

To address the transforming potential of *NUP98-KMT2A*, we cloned a full-length human fusion ORF into the *p2LOX* targeting-vector to integrate it into the *Hprt* gene locus on the X-chromosome under the control of a doxycycline-responsive element in embryonic stem cells. A reverse Tet transactivator (*rtTA*) stably integrated in the

Rosa26 locus allows doxycycline-regulated transgene expression (Figure 1A).[19,22,23] We used primarily female mice to mitigate the effects of any potential sex-related differences in transgene expression.

Induction of *iNUP98-KMT2A* results in an myelodysplastic syndrome-like disease *in vivo*

Primary-induced iNUP98-KMT2A mice developed signs of distress after a variable latency of 13-106 weeks (median latency=80 weeks, n=22) (Figure 1B). Blood values from non-induced iNUP98-KMT2A mice did not differ significantly from those of WT mice (*Online Supplementary Figure S1A*). We also explored disease induction by transplanting total BM from naïve (off doxycycline) iNUP98-KMT2A mice into lethally irradiated syngenic WT mice. In comparison to primary-induced mice, BM transplant recipient animals developed the symptoms earlier (median latency=32 weeks, *P*=0.0007, log-rank test, n=5) (Figure 1B, *Online Supplementary Table S3*).

Most symptomatic primary-induced iNUP98-KMT2A mice had peripheral blood counts in the normal range with slightly increased numbers of white blood cells, and reticulocytes. Decreases were seen in hemoglobin levels and red blood cell numbers (*P*=0.049, unpaired *t*-test, n=15) (Figure 1C). Blood values from iNUP98-KMT2A BM transplant recipients revealed a similar trend to those of primary-induced samples in all parameters analyzed with significantly increased numbers of white blood cells (*P*=0.0006, unpaired *t*-test, n=5) and reduced cellular hemoglobin levels (*P*=0.03, unpaired *t*-test, n=5). Notably, the overall cellularity of the BM of primary-induced mice was reduced (*P*=0.0099, unpaired *t*-test, n=9) relative to controls. Further analysis of different BM subpopulations revealed decreased numbers of myeloid cells (Mac-1$^+$/Gr-1$^+$), B cells (B220$^+$), and T cells (CD3$^+$) (*Online Supplementary Figure S1B*). Signs of intramedullary apoptotic cell death was found in some but not all mice as measured by combined PO-PRO-1 and 7-aminoactinomycin D staining (Figure 1C) with non-significant increased apoptosis of CD71$^+$Ter119$^+$, but not of myeloid (Mac-1$^+$, Gr-1$^+$) or lymphoid (CD3$^+$/CD8$^+$/B220$^+$) cells from primary-induced animals relative to WT controls (*Online Supplementary Figure S1C*). In primary induced mice we occasionally observed signs of dysplasia on blood smears, with the appearance of bi-lobed myeloid cells and polychromatophilic reticulocytes (Figure 1D) as well as signs of extramedullary hematopoiesis in the spleen and the liver (Figure 1E).

The BM of iNUP98-KMT2A mice that had been on doxycycline for several months displayed rather heterogeneous immunophenotypes: some showed an increase in Mac-1$^+$/Gr-1$^+$ cells, whereas others showed a marked decrease in mature myeloid cells with concomitant increases in FcγRII/III$^+$ and c-Kit$^-$ populations (Figure 1F, G).

To address potential reversibility, we transplanted iNUP98-KMT2A BM cells into lethally-irradiated WT recipients on doxycycline: upon development of symptoms in the first mouse, we reverted to non-doxycycline chow and followed the remaining mice for several months. Disease-free survival was significantly increased by the removal of doxycycline food (median latency=49 weeks, *P*=0.002, log-rank test, n=6) (Figure 1B) although analysis of peripheral blood at death revealed that many parameters remained similar to those of BM transplant recipients on doxycycline until death (Figure 1C).

Collectively, these data show that transgenic expression of *iNUP98-KMT2A* alters the hematopoietic system *in vivo*: there were increases in the numbers of white blood cells and apoptotic cells, and decreases in hemoglobin and the numbers of red blood cells and cells in the BM with signs of extramedullary hematopoiesis and morphological signs of dysplasia with some interindividual differences.

Expression of *iNUP98-KMT2A* leads to expansion and competitive advantage of hematopoietic stem and progenitor cells

We next studied the impact of *iNUP98-KMT2A* expression on the cellular hierarchy of the BM. We found that prior to developing symptoms (mean time on doxycycline: 36 weeks), iNUP98-KMT2A mice displayed an expansion of Lin$^-$ Sca-1$^+$ c-Kit$^+$ (LSK) hematopoietic stem and progenitor cells (HSPC) (*P*=0.04, unpaired *t*-test, n=4) (Figure 2A, *Online Supplementary Figure S1D*). Further breakdown of the LSK compartment revealed no significant changes in the relative distribution of CD34$^-$ long-term hematopoietic stem cells, and CD34$^+$, CD48$^+$, CD150$^-$ multipotent progenitors (Figure 2B). Interestingly, we found that iNUP98-KMT2A LSK, but not mature cells, from asymptomatic mice (mean time on doxycycline: 55 weeks) were cycling more than control cells as shown by a reduced fraction of quiescent cells in G_0 phase (*P*=0.0098, unpaired *t*-test, n=3) and an increase in the G_1 fraction (Figure 2C, *Online Supplementary Figure S1E*).

To address the functional consequence of the increased LSK number in iNUP98-KMT2A mice on doxycycline, we performed competitive repopulation assays. Naïve CD45.2$^+$ iNUP98-KMT2A or WT (CTRL) total BM cells were transplanted 1:1 with CD45.1$^+$ WT total BM cells into lethally-irradiated CD45.1$^+$ WT recipients (on doxycycline) and the cellular chimerism in the peripheral blood was determined 4, 8, 12, 18, and 25 weeks after transplantation. We observed that the proportion of CD45.2$^+$ iNUP98-KMT2A cells in the peripheral blood steadily increased over time (Figure 2D) whereas the chimerism in mice that received CD45.2$^+$ WT BM cells did not change significantly, remaining near to 50%. The percentage of iNUP98-KMT2A CD45.2$^+$ cells was initially lower than that of CTRL (WT) (*P*=0.0153, *t*-test, n=5). After 18 weeks, CD45.2$^+$ iNUP98-KMT2A cell numbers had increased by 1.6-fold compared to week 4 (*P*=0.034, *t*-test, n=5) and by 25 weeks CD45.2$^+$ iNUP98-KMT2A cell numbers had further increased relative to initial measurements (*P*=0.004, *t*-test, n=5) and were 20% greater than CD45.2$^+$ WT cells at the same time-point [*P*=0.019, 2-way analysis of variance (ANOVA), n=4]. Interestingly, iNUP98-KMT2A CD45.2$^+$ cells contributed to a greater extent to the myeloid lineage (Gr-1$^+$) and the B lineage (B220$^+$) but equally to the T lineage (CD3$^+$), compared to WT controls (Figure 2E). Transplantation of total BM from primary recipients into lethally-irradiated CD45.1$^+$ secondary recipients resulted in a heterogeneous outcome: in two mice ("M1" & "M2") the BM was dominated by CD45.2$^+$ cells, while two other mice ("M4" & "M5") showed predominantly CD45.1$^+$ cells. One mouse ("M3") developed a CD45.2$^+$ AML 23 weeks after transplantation (Figure 2F).

Some iNUP98-KMT2A mice develop transplantable acute myeloid leukemia

After a median latency of 62 weeks, six out of 22 iNUP98-KMT2A mice on doxycycline developed a

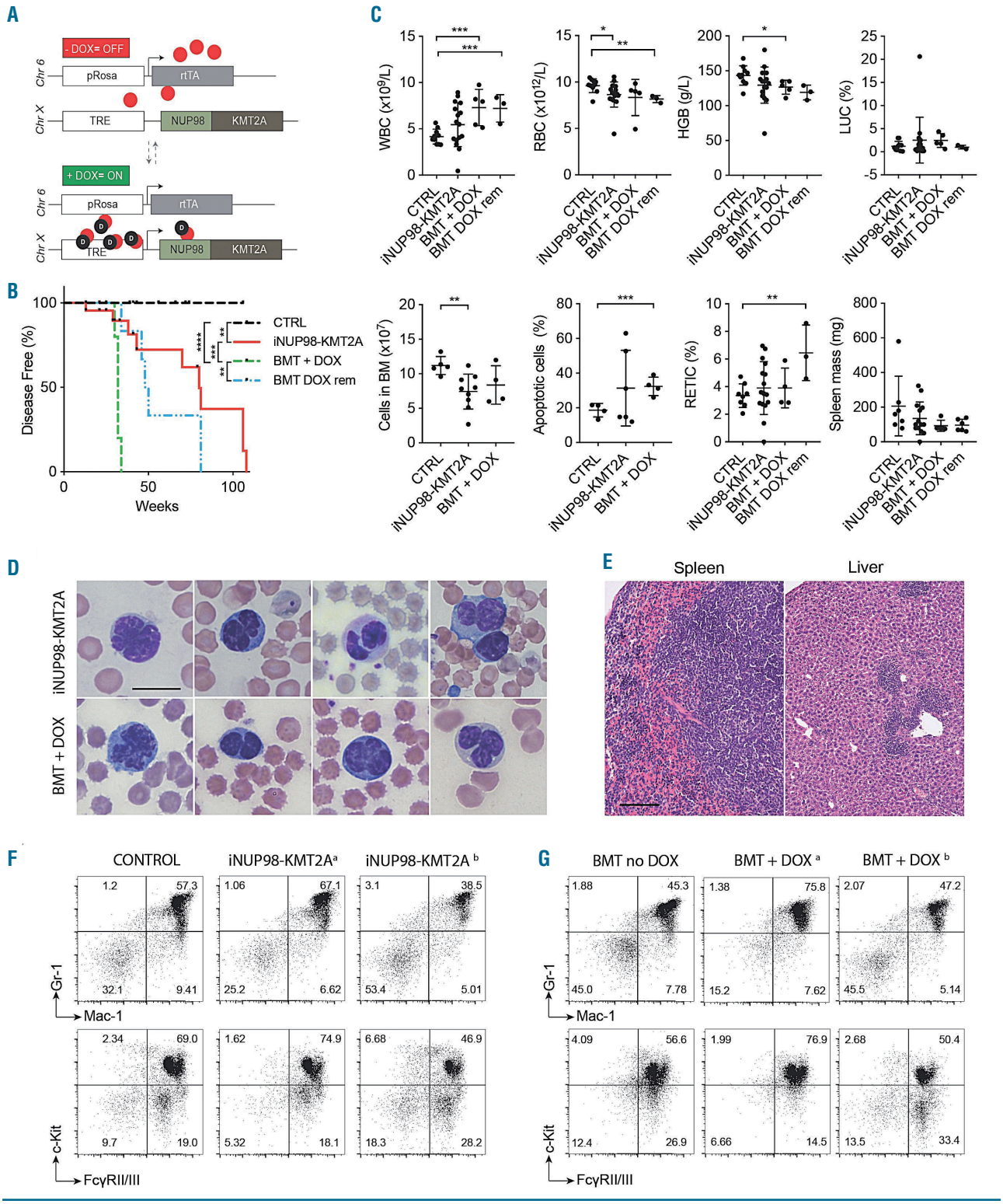

Figure 1. Expression of *iNUP98-KMT2A* leads to development of a myelodysplastic syndrome-like disease in transgenic mice. (A) iNUP98-KMT2A mice contain a reverse Tet transactivator (*rtTA*) element in the *Rosa26* gene locus on chromosome 6 (Chr 6), and a human *NUP98-KMT2A* open reading frame after a TET-responsive element (TRE) in the *Hprt* locus on the X-chromosome (Chr X). Administration of the tetracycline analog, doxycycline (DOX) leads to expression of the *NUP98-KMT2A* fusion construct. (B) Kaplan-Meier curves for DOX-exposed primary-induced adult (6-10 weeks) iNUP98-KMT2A mice and wildtype (WT) littermates (CTRL), as well as adult WT irradiated recipients of iNUP98-KMT2A total bone marrow transplants (BMT) exposed to DOX (BMT + DOX) and BMT recipients taken off DOX (BMT DOX rem) after 31 weeks. **P*<0.05, ***P*<0.01, ****P*<0.001, *****P*<0.0001, log-rank test. (C) Blood values from DOX-exposed adult iNUP98-KMT2A mice and WT littermates (CTRL), as well as adult WT irradiated recipients of iNUP98-KMT2A total BMT exposed to DOX (BMT + DOX) and BMT recipients taken off DOX (BMT DOX rem) after 31 weeks. **P*<0.05, ***P*<0.01, ****P*<0.001, unpaired *t*-tests. WBC: white blood cells; RBC: red blood cells; HGB: hemoglobin; LUC: abnormal leukocytes. (D) Dysplastic immature myeloid cells on peripheral blood smears of pre-leukemic DOX-induced iNUP98-KMT2A mice as well as WT recipients of iNUP98-KMT2A total BMT on DOX. Scale bar: 10 μm. (E) Histopathology sections of DOX-exposed iNUP98-KMT2A mice show extramedullary hematopoiesis in the spleen and liver. Scale bar: 100 μm. (F) Immunophenotype (Mac-1, Gr-1, FcγRII/III and c-Kit, given in %) of total bone marrow cells from pre-leukemic iNUP98-KMT2A mice. The flow plots are representative of three mice/group. (G) Immunophenotype (Mac-1, Gr-1, FcγRII/III and c-Kit, given in %) of total bone marrow cells from WT mice transplanted with iNUP98-KMT2A bone marrow on DOX. Mice exhibited two diverse phenotypes; denoted *a* and *b*. Transplanted mice off DOX were used as the negative control.

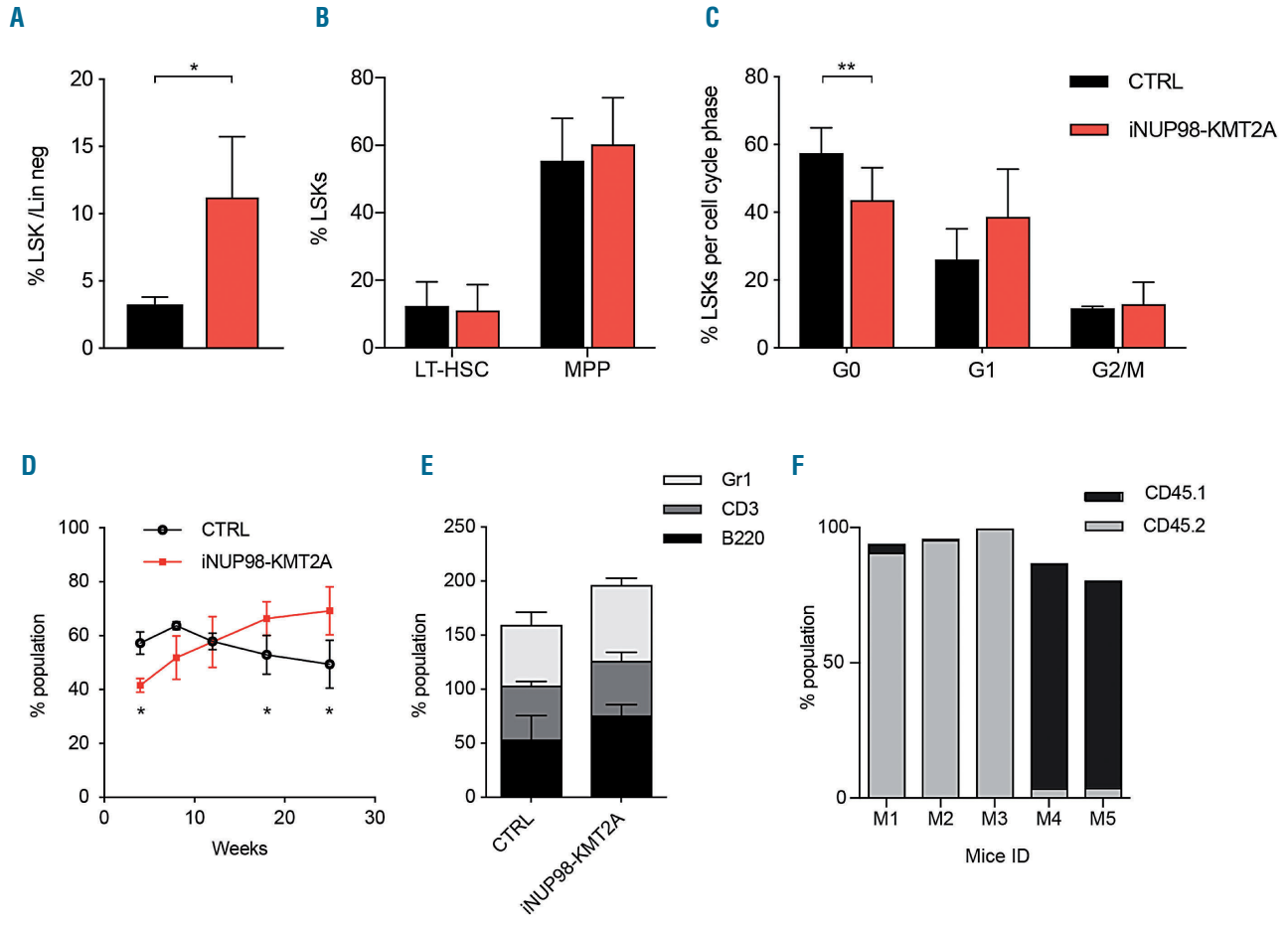

Figure 2. Expression of *iNUP98-KMT2A* results in LSK cell expansion with a competitive repopulation advantage. (A) Lineage negative (Lin^-) bone marrow (BM) cells from pre-leukemic iNUP98-KMT2A mice and wildtype (WT) littermate controls (CTRL) were stained for c-Kit and Sca-1 and analyzed by flow cytometry. *P<0.05, unpaired t-test. (B) Lin^- BM from pre-leukemic iNUP98-KMT2A mice and WT littermate controls were stained for markers of long-term hematopoietic stem cells (LT-HSC) (LSK, $CD150^+$, $CD48^-$) and multipotent progenitors (MPP) (LSK, $CD34^+$, $CD48^+$, $CD150^-$) and analyzed by flow cytometry. The percentages of LSK identified as LT-HSC and MPP are shown. (C) Cell cycle analysis of LSK from pre-leukemic iNUP98-KMT2A mice and WT littermate controls. **P<0.01, unpaired t-test. (D) Competitive repopulation assay: lethally-irradiated CD45.1 WT recipients were transplanted with a 1:1 mixture of total BM cells from CD45.2 iNUP98-KMT2A and CD45.1 WT mice in the presence of doxycycline (DOX). The percentage of CD45.2 cells present in the peripheral blood was measured by flow cytometry over a period of 25 weeks. *P<0.05, unpaired t-test. (E) At week 25 of the competitive repopulation assay, the $CD45.2^+$ cells were analyzed for percentages of Gr-1, CD3, and B220 markers. (F) Cellular BM chimerism of WT $CD45.1^+$ mice 25 weeks after competitive transplantation with $CD45.2^+$ iNUP98-KMT2A BM. All mice were exposed to DOX throughout the experiment.

leukemic phenotype characterized by the presence of leukemic blasts on peripheral blood smears, and extensive leukemic infiltration in the BM, spleen, liver and lungs (Figure 3A, *Online Supplementary Figure S2A*). This was accompanied by significantly increased white blood cell counts (P=0.0018, unpaired t-test, n=5) and abnormal leukocytes ("LUC") (P=0.0468, unpaired t-test, n=5) counts in the periphery and splenomegaly (Figure 3B, *Online Supplementary Table S4*). Immunophenotypic analysis of highly-infiltrated BM revealed intermediate to high expression levels of myeloid markers Mac-1, Gr-1, and FcγRII/III in five out of six mice, with baseline expression of B220 and CD3 lymphoid markers characterizing the disease as AML (Figure 3C, *Online Supplementary Figure S2B-D*).

Transplantation of total BM from diseased mice into sublethally-irradiated WT mice induced disease in 100% of recipients. Whereas disease development was fully doxycycline-dependent upon transplantation of AML cells from one donor ("M1") (median latency 28 weeks, P=0.025, log-rank test, n=4), leukemic cells from another donor ("M2") resulted in disease in all recipients regardless of doxycycline administration, with a similar latency (26-37 weeks) to that of recipients of "M1" cells on doxycycline (Figure 3D). Flow cytometric analysis of BM samples from transplanted leukemic mice revealed heterogeneity in M1 ("M1a" & "M1b") BM recipients, including a marked doxycycline-dependent increase in $CD3^+$ cells, but a consistent myeloid phenotype in recipients of M2 (Figure 3E).

Given the long latency to develop primary disease, we explored whether additional genotoxic insults might accelerate disease induction. Indeed, sublethal γ-irradiation (1x 600 cGy) of asymptomatic 3- to 4-week old iNUP98-KMT2A mice on doxycycline resulted in earlier onset of disease symptoms than that observed in sublethally-irradiated WT mice (median latency 26 weeks *vs.* undefined; P=0.032, log-rank test, n=5) (Figure 3F, *Online*

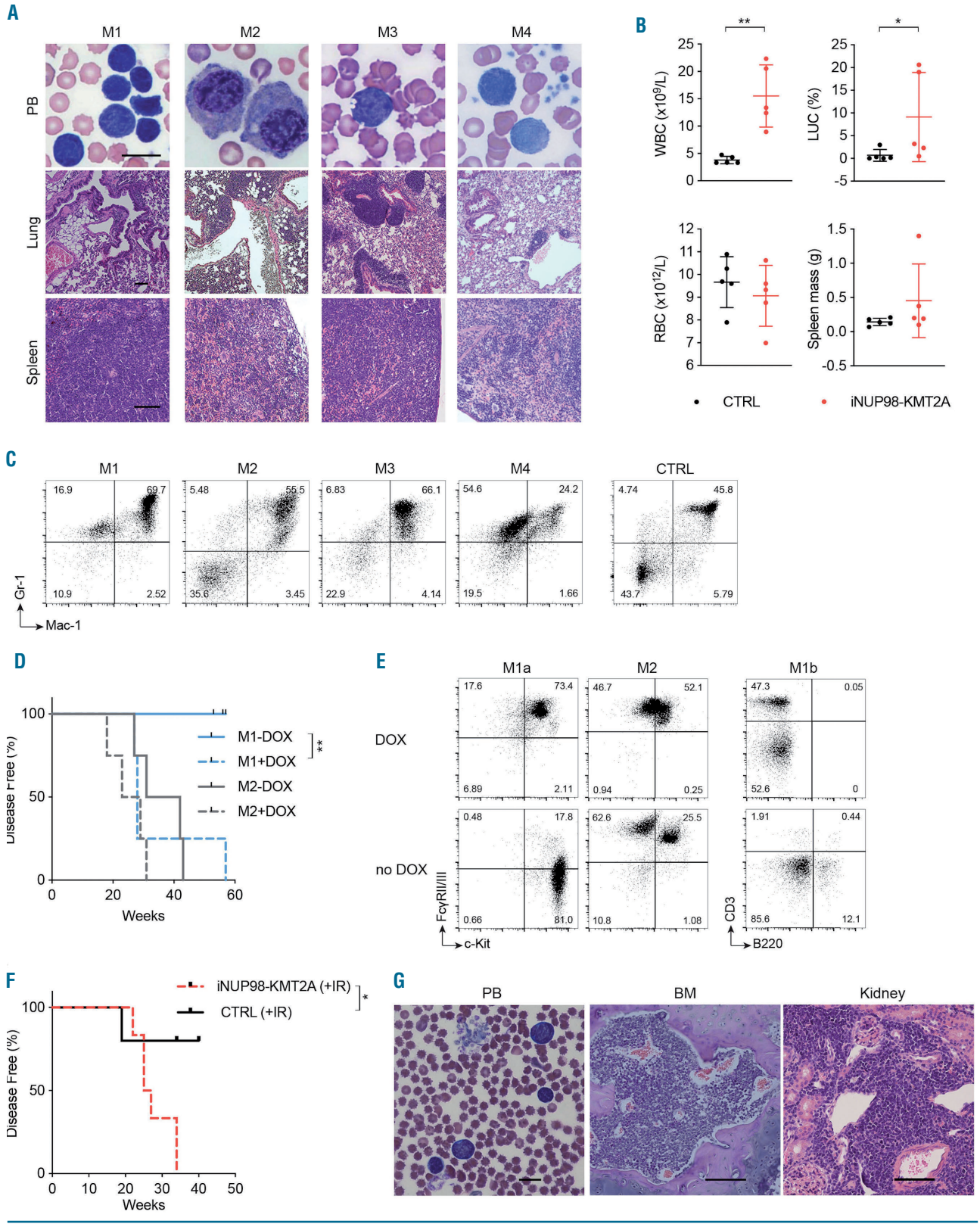

Figure 3. Expression of *iNUP98-KMT2A* induces a transplantable acute myeloid leukemia in some mice. (A) Histological sections and peripheral blood (PB) smears from four leukemic iNUP98-KMT2A mice. Scale bar: 10 μm. (A) Blood values from doxycycline (DOX)-treated iNUP98-KMT2A mice which developed symptoms of leukemia as well as wildtype (WT) littermate controls (CTRL). **P*<0.05, ***P*<0.01, unpaired *t*-test, n=5. WBC: white blood cells; LUC: abnormal leukocytes; RBC: red blood cells. (C) Gr-1 and Mac-1 expression on total BM cells from leukemic iNUP98-KMT2A mice and a representative control mouse. (D) Total BM from leukemic mice M1 and M2 was transplanted into WT recipients in the presence or absence of DOX. Kaplan-Meier curves show disease-free survival of transplanted animals. ***P*<0.01, log-rank test. (E) Representative immunophenotypes of total BM of recipients (on DOX) (from Figure 3D) either transplanted with iNUP98-KMT2A acute myeloid leukemia from mouse M1: M1a and M1b; or from mouse M2. (F) iNUP98-KMT2A mice were exposed to DOX 48 h prior to sublethal irradiation (600 cGy). Irradiated (IR) WT mice were used as controls. Kaplan-Meier curves illustrate disease-free survival. **P*<0.05, log-rank test. (G) Representative histopathology section of a symptomatic irradiated iNUP98-KMT2A mouse. The BM is infiltrated with blasts which are also visible in the peripheral blood (PB) and kidney. Scale bars: PB: 10 μm; BM & kidney: 100 μm.

Supplementary Table S5) and that seen in our cohort of primary-induced, non-irradiated iNUP98-KMT2A mice on doxycycline (median latency 26 *vs.* 80 weeks; *P*=0.0003, log-rank test, n=6) (*Online Supplementary Figure 3A*). All symptomatic mice had extensive multi-organ infiltration by leukemic blasts, which were visible on peripheral blood smears as well as in the BM and kidneys (Figure 3G). Collectively, these data show that expression of *iNUP98-KMT2A* leads to an MDS-like disease and in some cases to transplantable AML in mice.

Expression of *iNUP98-KMT2A* results in aberrant cell cycle progression and escape from senescence

In the presence of doxycycline (1 μg/mL), *ex vivo* proliferation of Lin$^-$ iNUP98-KMT2A BM cells was significantly impaired in liquid culture containing cytokines (murine stem cell factor, interleukin-6, and interleukin-3 (*Online Supplementary Figure S3B*). Expression of *iNUP98-KMT2A* was verified on day 6 of the culture (*Online Supplementary Figure S3C*). However, *iNUP98-KMT2A* expression did not significantly alter the clonogenic growth of BM cells in methylcellulose containing doxycycline (*Online Supplementary Figure S3D*). Cell cycle analysis of Lin$^-$ iNUP98-KMT2A BM cells challenged with doxycycline *in vitro* revealed an increase in the number of cells in G_1 phase (*P*=0.033, unpaired *t*-test, n=3) at the expense of G_0 and G_2/M phases (*P*=0.049, unpaired *t*-test, n=3) (*Online Supplementary Figure S3E*), similar to what was observed in LSK from iNUP98-KMT2A mice on doxycycline (Figure 2C).

To further explore the impact of *iNUP98-KMT2A* expression on cell cycle regulation we established MEF. We first verified *iNUP98-KMT2A* expression in the MEF (Figure 4A). We then determined cell cycle progression of iNUP98-KMT2A MEF on doxycycline and found accumulation of the cells in the G_1 phase (*P*=0.081, unpaired *t*-test, n=3) with a significant reduction of the percentage of cells in the G_2/M phase (*P*=0.029, unpaired *t*-test, n=3) (Figure 4B). Initially, both iNUP98-KMT2A and WT MEF grew at similar rates; however, upon serial propagation of the cells we observed reduced growth of WT MEF with signs of senescence (visualized by X-gal staining for senescence-associated β-galactosidase activity) after 10-13 passages (Figure 4C, *Online Supplementary Figure S3F, G*). In contrast, iNUP98-KMT2A MEF continued to grow at an increased rate (*P*=0.0156, Wilcoxon matched-pairs signed rank test, n=2) up to, and beyond, passage 40. To understand how iNUP98-KMT2A MEF escape senescence, we compared the expression of 84 genes related to cell cycle regulation and senescence using a commercial array-based reverse transcription PCR assay. Combining two independent experiments revealed no significant changes in gene expression at an early time-point (passage 1) (Figure 4D) while the levels of expression of eight genes were significantly reduced in iNUP98-KMT2A MEF relative to WT MEF at later passages (passage 10-13) (Figure 4E).

Genes that were found to be dysregulated in late-passage iNUP98-KMT2A MEF samples were further analyzed in iNUP98-KMT2A HSPC, which had been exposed to doxycycline *in vitro* for 48 h. Expression patterns observed in MEF for *Sirt1*, *Rbl2*, *Twist1*, *Prkcd*, *Vim*, and *Tert* were found to be similar in iNUP98-KMT2A HSPC, demonstrating common patterns of gene regulation in MEF and primary iNUP98-KMT2A cells (Figure 4F).

iNUP98-KMT2A$^+$ acute myeloid leukemia cells do not express the *HoxA-B-C* gene cluster and are resistant to compounds targeting the KMT2A-menin interaction

In contrast to other NUP98 fusions, primary patients' NUP98-KMT2A AML cells were shown to express reduced levels of the *HOXA-B-C* gene cluster.[19] Likewise, leukemic blasts from diseased *iNUP98-KMT2A* mice generally expressed very low levels of *HoxA5*, *HoxA9*, *HoxA10*, *HoxB4*, *HoxB6*, *HoxC6* and *HoxC9* mRNA compared to normal BM cells or to leukemic blasts transformed by retroviral *KMT2A-ENL* (*rKMT2A-ENL*) or the *rKMT2A-AF9* fusion genes (Figure 5A).[24]

The lack of *KMT2A* exon 1 encoding for the very N-terminus, which mediates the menin/LEDGF interaction, predicts that cells carrying the NUP98-KMT2A fusion protein would be resistant to small molecule menin inhibitors. However, if leukemic transformation by NUP98 fusions depends on KMT2A, as suggested by recent studies,[14,25] NUP98-KMT2A leukemic blasts might be susceptible to inhibition by small molecules targeting critical KMT2A functional interactions. To address this question, we exposed cells from two leukemic iNUP98-KMT2A mice ("M1" & "M3") to different doses of the small molecule menin inhibitor (MI-2-2) and to a bromodomain inhibitor blocking BET-family proteins including BRD4 (JQ1) previously shown to efficiently block KMT2A and KMT2A-fusion controlled transcription.[26] As shown in Figure 5B, MI-2-2 (3-12 μM) did not impair growth of iNUP98-KMT2A leukemic blasts but at 6 μM and 12 μM induced a G_1 cycle arrest in leukemic cells expressing the rKMT2A-AF9 fusion (*P*<0.0001, two-way ANOVA, n=2), with a concomitant decrease in the proportion of cells in the S-phase (*P*<0.0001, two-way ANOVA, n=2) and in the G_2/M-phase (6 μM: *P*=0.0246; 12 μM: *P*=0.0144, two-way ANOVA, n=2). Exposure of iNUP98-KMT2A cells to low (0.05-0.5 μM) doses of JQ1 did not induce cell cycle arrest or significant cytotoxicity as seen in rKMT2A-AF9 cells (Figure 5C), but increased the fraction of cells in the G_1 phase of the cycle, suggesting alternative transforming mechanisms of NUP98-KMT2A compatible with a defective cell cycle checkpoint control.

Discussion

Inv(11)(p15q23) has been reported in a heterogeneous group of human hematologic malignancies including MDS, AML, peripheral T-cell lymphoma, childhood acute lymphoblastic acute leukemia, myeloma and hairy cell leukemia.[20] In the majority of the myeloid cases, inv(11)(p15q23) was the sole cytogenetic abnormality, suggesting a role as a leukemogenic driver. Expression of a *NUP98-KMT2A* fusion gene has so far been reported in two AML patients with inv(11)(p15q23).[19] Detailed molecular work-up of additional patients is needed to delineate the epidemiology of this rare entity. Notably, inv(11)(p15q23) was also found in some solid cancers but never analyzed in more detail.[20] To determine the transforming potential of the *NUP98-KMT2A* fusion gene we developed inducible transgenic mice. This approach avoids some of the drawbacks of retroviral gene transfer such as cooperating integration events or transduction bias of early myeloid progenitor cells. In addition, the large size of the *NUP98-KMT2A* fusion ORF would clear-

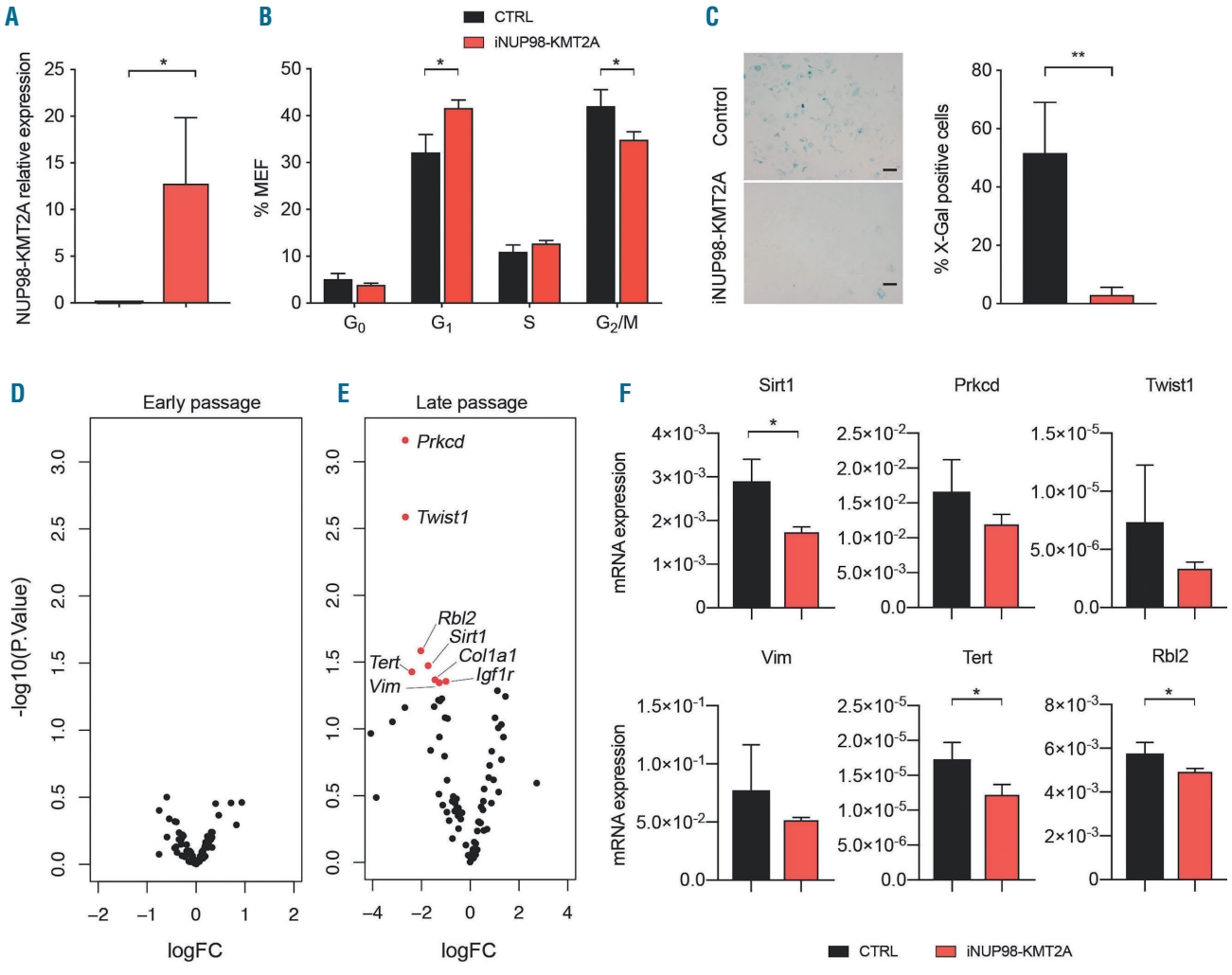

Figure 4. *iNUP98-KMT2A* expression impairs cell cycle progression of murine embryonic fibroblasts and bone marrow-derived hematopoietic stem and progenitor cells. (A) Murine embryonic fibroblasts (MEF), derived from iNUP98-KMT2A and wildtype (WT) control (CTRL) littermate mice were cultured in vitro in the presence of doxycycline (DOX) (1 μg/mL). *iNUP98-KMT2A* expression is shown relative to the level of *GAPDH* expression. **P*<0.05, unpaired *t*-test, n=3. (B) Flow cytometry-based cell cycle analysis showed increased G_1 and decreased G_2/M fractions of *in vitro*-cultured iNUP98-KMT2A+ MEF compared to WT controls. **P*<0.05, unpaired *t*-test, n=3. (C) iNUP98-KMT2A and WT MEF cultured for eight passages in the presence of DOX (1 μg/mL) were stained for senescence-associated B-galactosidase activity with X-Gal (left panel). The number of X-Gal$^+$ cells in the culture was quantified (right panel). Images and counts are representative of three biological replicates. Scale bars: 100 μm. ***P*<0.01, unpaired t-test, n=3. (D) Differential mRNA expression from early (passages 1-2) and late (passages 8-10) passaged WT and iNUP98-KMT2A MEF analyzed by a RT2 PCR array. Significant (*P*<0.05) changes are highlighted in red. (E) Validation of differentially expressed genes in MEF (Figure 4D) by quantitative polymerase chain reaction analysis in WT and iNUP98-KMT2A hematopoietic stem and progenitor cells after exposure to DOX (1 μg/mL) *in vitro* for 48 h. *<0.05, unpaired *t*-test, n=3.

ly limit the generation of high-titer retroviral particles. We used a doxycycline-regulated transgenic expression system in which the *rtTA* is integrated into the ubiquitously expressed *Rosa26* locus and the *NUP98-KMT2A* fusion is in the *Hprt* locus under control of a tet-responsive minimal promoter, previously used to model the impact of cellular origin in *KMT2A-AF9* and *KMT2A-ENL*-driven leukemia.[22,23,27]

Secondary transplantation of iNUP98-KMT2A leukemic cells revealed that the inherent leakiness of the system might be sufficient to drive the phenotype in the absence of doxycycline after cellular selection in the mouse (Figure 3D) suggesting that, in contrast to *KMT2A-AF9* or *KMT2A-ENL*, low level *NUP98-KMT2A* transgene expression is sufficient to exert its oncogenic activity or that expression of the transgene might be required for initial transformation but not for maintenance of neoplastic cells in all cases.

Retroviral expression, as well as constitutive or conditional activation, of many AML-associated fusions [involving the retinoic acid receptor alpha (RARA), core binding factor (CBF) or KMT2A] in the hematopoietic system of the mouse often closely phenocopies human disease.[28,29] In most of these models, AML develops after a long latency without evidence of a symptomatic pre-leukemic MDS phase, with few exceptions such as the *Vav1*-promoter driven *NUP98-HOXD13* fusion.[30] NUP98-HOXD13 mice developed T-cell leukemia, undifferentiated leukemia, megakaryocytic and erythroid leukemia or symptomatic MDS. In contrast, iNUP98-KMT2A mice (5 out of 22) only developed Gr-1$^+$/Mac-1$^+$/c-Kit$^+$ AML. Leukemic transformation of NUP98-HOXD13 mice was

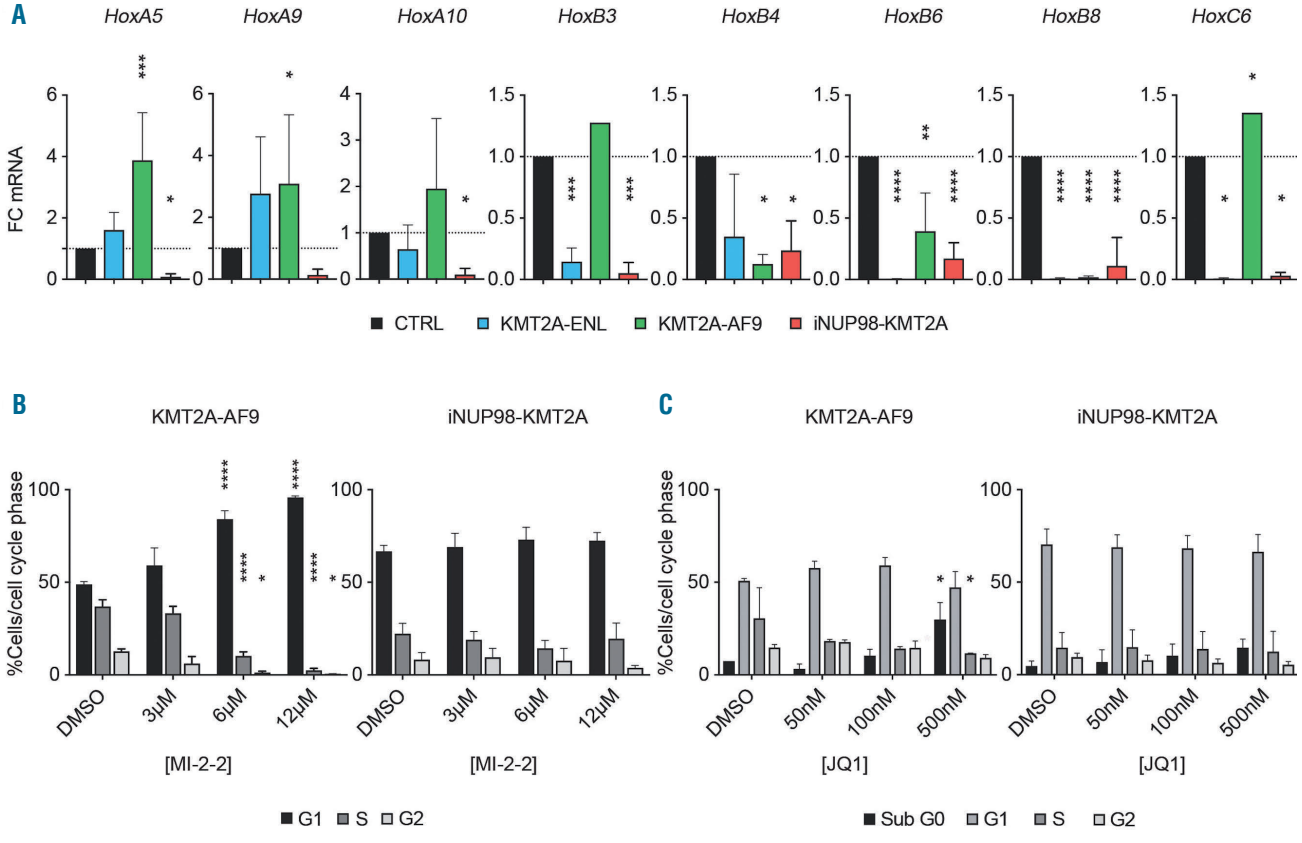

Figure 5. iNUP98-KMT2A acute myeloid leukemia cells express low levels of *Hox* genes and are resistant to small molecule menin and Brd4 inhibitors. (A) Expression of *HoxA*, *-B*, and *-C* genes was quantified by quantitative polymerase chain reaction (qPCR) analysis in total bone marrow from wildtype (WT) control (CTRL) cells, leukemic cells from iNUP98-KMT2A mice as well as from mice transplanted with retrovirally-transduced KMT2A-ENL (rKMT2A-ENL) and rKMT2A-AF9 cells. Expression relative to that of WT cells is shown. **P*<0.05, ***P*<0.01, ****P*<0.001, *****P*<0.0001, one-way analysis of variance (ANOVA) relative to control, n=3. (B) rKMT2A-AF9 and iNUP98-KMT2A leukemic blasts were treated with the menin inhibitor, MI-2-2, for 48 h at the indicated concentrations and the cell cycle phase was analyzed by flow cytometry. The figure shows the percentage of cells in each phase of the cell cycle. **P*<0.05, ***P*<0.01, ****P*<0.001, *****P*<0.0001, two-way ANOVA relative to cells treated with dimethylsulfoxide (DMSO), n=2. (C) rKMT2A-AF9 and iNUP98-KMT2A leukemic blasts were treated with the BRD4 inhibitor, JQ1, for 48 h at the indicated concentrations. Cell cycle phase was analyzed by flow cytometry. The figure shows the percentage of cells in each phase of the cell cycle. **P*<0.05, two-way ANOVA relative to DMSO-treated cells, n=2.

accompanied by spontaneous mutations in *Nras*, *Kras* and *Cbl*; however, no such mutations were found in three iNUP98-KMT2A mice that developed AML[31] *(data not shown)*. Several studies also demonstrated leukemogenic cooperation of NUP98-HOXD13 with overexpression of *Meis1*, *MN1*, or loss of *p53* or *p15*^{INK4B}.[32-35] Intercrossing of transgenic NUP98-HOXD13 mice with *Flt3*-internal tandem duplication (ITD) knock-in mice resulted in acceleration to a fully-penetrant AML phenotype.[36] In contrast to NUP98-HOXD13, we observed that transplantation of iNUP98-KMT2A BM cells retrovirally overexpressing *FLT3*-ITD did not accelerate the disease (*data not shown*).[36]

In the presence or absence of *FLT3*-ITD, pre-leukemic NUP98-HOXD13 cells expressed significantly increased levels of *HoxA7*, *HoxA9*, *HoxB4*, *HoxB6*, *HoxB7*, *HoxC4* and *HoxC6* mRNA.[30,36] In sharp contrast, BM cells from diseased iNUP98-KMT2A mice expressed significantly reduced levels of the *HoxA-B-C* gene cluster compared to normal BM cells, recapitulating what was shown in primary NUP98-KMT2A$^+$ AML cells.[19] Expression levels of *HoxA-B-C* genes below those observed in normal HSPC suggest that the iNUP98-KMT2A fusion may affect the function of normal KMT2A in a dominant-negative manner.

Previous work showed that KMT2A plays a critical role in cell cycle progression.[37] Interestingly, under baseline conditions, we found a higher proportion of iNUP98-KMT2A Lin$^-$ cells in S-phase when compared to WT cells supporting previous studies indicating that ablation of normal KMT2A function results in defective S-phase cell cycle entry. The percentage of both WT and iNUP98-KMT2A cells in S-phase decreased following exposure to ionizing radiation (*data not shown*) as has been demonstrated previously.[38] Interestingly, compared to control cells, *in vitro* doxycycline treatment of both iNUP98-KMT2A BM-derived HSPC and MEF led to the accumulation of cells in the G_1-phase, mirroring what was seen in LSK cells taken from iNUP98-KMT2A mice that had been on doxycycline food for several months. Further experiments with MEF showed that expression of *iNUP98-KMT2A* abrogated cellular senescence: compared to WT cells, iNUP98-KMT2A MEF on doxycycline never showed any signs of crisis and could easily be propagated for >45 passages. In contrast, iNUP98-KMT2A cells off doxycycline showed signs of a crisis at passages 10-12 but were able to escape and could also be propagated for over 40 passages (*data not shown*), suggesting that very low expression of *iNUP98-KMT2A* is suffi-

cient to provide the cells the signals to escape apoptosis after crisis.

Among the genes downregulated in late passage iNUP98-KMT2A relative to control MEF, many have been implicated in cell cycle- or senescence-regulatory capacities. Previously, *sirtuin1* (*sirt1*)-deficient MEF were shown to be resistant to replicative senescence through a p53-dependent mechanism;[39] there is also evidence to suggest that Sirt1 plays a crucial role in Foxo3-activated cell cycle arrest.[40] It has been shown that the insulin-like growth factor 1 receptor (IGF1R) ligand, insulin-like growth factor (IGF1), is involved in cellular senescence control through the Sirt1-p53 axis,[41] in line with a proposed model whereby p53-dependent cellular senescence is counteracted by inhibition of IGF1R signaling.[42] In a lung fibroblast cell model, Rbl2 (p130) expression was increased along with E2F-4 and markers of cellular senescence following heat shock protein-27 (HSP27) knock-down. Inhibition of Rbl2 counteracted the effects of HSP27 knock-down and significantly reduced senescence-associated β-galactosidase staining in a p53-independent manner.[43] Additionally, the ribonuclease polymerase Tert (telomerase reverse transcriptase), which maintains telomeric ends, has a well-demonstrated role in resisting senescence; however, some primary tumor samples have tested negative for telomerase activity[44] and alternative mechanisms to overcome replication-associated telomeric shortening have been proposed with evidence for alternative lengthening of telomeres in 10-15% of cancers.[45] Finally, the role of protein kinase C delta (Prkcd) in senescence is currently poorly understood, but studies have suggested that Prkcd is an important mediator of transforming growth factor-β-induced senescence.[46]

Peptides and small molecule antagonists of KMT2A-menin/LEDGF interactions have been shown to reduce the transforming activity of KMT2A fusions by interfering with binding to targets, including the *HOX-A* gene cluster.[5-10] It has been shown that leukemic transformation by NUP98 fusions is KMT2A-dependent;[14] this would support the idea that iNUP98-KMT2A AML cells are susceptible to small molecules targeting the N-terminus of WT KMT2A. Conversely, the lack of the menin/LEDGF interaction site would predict poor sensitivity of iNUP98-KMT2A AML cells to these compounds. Indeed, compared to KMT2A-AF9-driven cells, iNUP98-KMT2A leukemic cells were resistant to blockade of the KMT2A-menin interaction by the small molecule MI-2-2 at concentrations previously demonstrated to inhibit growth of human KMT2A-AF4 and murine KMT2A-AF9 transformed cells.[12,47] iNUP98-KMT2A AML cells also showed a reduced sensitivity to the BET-bromodomain inhibitor JQ1, which interferes with active transcription and elongation through displacement of BRD4 from chromatin,[48] while challenge of KMT2A-AF9 cells recapitulated published growth inhibition.[26] This suggests that targeting KMT2A might not be suitable for efficient therapeutic interference with NUP98-KMT2A AML.

Acknowledgments

The authors thank Danny Labes, Telma Lopes, Emmanuel Traunecker, and Lorenzo Raeli from the University of Basel Flow Cytometry Facility; Nicole Meier and the members of the Animal Care Facility at the University of Basel; Masao Seto for the full-length human KMT2A mRNA; Michael Kyba for providing the A2Lox-Cre ES cells; and Patrick Kopp and Jean-Françoise Spetz for their assistance generating the iNUP98-KMT2A mice.

Funding

JS's laboratory was supported by: grants from Swiss Cancer Research (KFS-4258-08-2017, KFS-3487-08-2014) and the Swiss National Science Foundation (SNF, 31003_A_173224/1). AP was supported by the Novartis Research Foundation. Basel, Switzerland.

References

1. Gough SM, Slape CI, Aplan PD. NUP98 gene fusions and hematopoietic malignancies: common themes and new biologic insights. Blood. 2011;118(24):6247-6257.
2. Takeda A, Yaseen NR. Nucleoporins and nucleocytoplasmic transport in hematologic malignancies. Semi Cancer Biol. 2014;27:3-10.
3. Muntean AG, Hess JL. The pathogenesis of mixed-lineage leukemia. Annu Rev Pathol. 2012;7:283-301.
4. de Boer J, Walf-Vorderwulbecke V, Williams O. In focus: MLL-rearranged leukemia. Leukemia. 2013;27(6):1224-1228.
5. Yokoyama A. Transcriptional activation by MLL fusion proteins in leukemogenesis. Exp Hematol. 2016;46:21-30.
6. Slany RK. The molecular mechanics of mixed lineage leukemia. Oncogene. 2016; 35:5215-5223.
7. Murai MJ, Chruszcz M, Reddy G, Grembecka J, Cierpicki T. Crystal structure of menin reveals binding site for mixed lineage leukemia (MLL) protein. J Biol Chem. 2011;286(36):31742-31748.
8. Huang J, Gurung B, Wan B, et al. The same pocket in menin binds both MLL and JUND but has opposite effects on transcription. Nature. 2012;482(7386):542-546.
9. Yokoyama A, Somervaille TC, Smith KS, Rozenblatt-Rosen O, Meyerson M, Cleary ML. The menin tumor suppressor protein is an essential oncogenic cofactor for MLL-associated leukemogenesis. Cell. 2005;123 (2):207-218.
10. Yokoyama A, Cleary ML. Menin critically links MLL proteins with LEDGF on cancer-associated target genes. Cancer Cell. 2008;14(1):36-46.
11. Grembecka J, He S, Shi A, et al. Menin-MLL inhibitors reverse oncogenic activity of MLL fusion proteins in leukemia. Nat Chem Biol. 2012;8(3):277-284.
12. Borkin D, Pollock J, Kempinska K, et al. Property focused structure-based optimization of small molecule inhibitors of the protein-protein interaction between menin and mixed lineage leukemia (MLL). J Med Chem. 2016;59(3):892-913.
13. Pascual-Garcia P, Jeong J, Capelson M. Nucleoporin Nup98 associates with Trx/MLL and NSL histone-modifying complexes and regulates Hox gene expression. Cell Rep. 2014;9(2):433-442.
14. Xu H, Valerio DG, Eisold ME, et al. NUP98 fusion proteins interact with the NSL and MLL1 complexes to drive leukemogenesis. Cancer Cell. 2016;30(6):863-878.
15. Shima Y, Yumoto M, Katsumoto T, Kitabayashi I. MLL is essential for NUP98-HOXA9-induced leukemia. Leukemia. 2017;31(10):2200-2210.
16. Mitani K, Sato Y, Hayashi Y, et al. Two myelodysplastic syndrome cases with the inv(11)(p15q23) as a sole chromosomal abnormality. Br J Haematol. 1992;81(4):512-515.
17. Inaba T, Hayashi Y, Hanada R, Nakashima M, Yamamoto K, Nishida T. Childhood myelodysplastic syndromes with 11p15 translocation. Cancer Genet Cytogenet. 1988;34(1):41-46.
18. Calabrese G, Fantasia D, Spadano A, Morizio E, Di Bartolomeo P, Palka G. Karyotype refinement in five patients with acute myeloid leukemia using spectral karyotyping. Haematologica. 2000;85(11):1219-1221.
19. Kaltenbach S, Soler G, Barin C, et al. NUP98-MLL fusion in human acute myeloblastic leukemia. Blood. 2010;116(13):2332-2335.
20. Huret JL. t(17;20)(q21;q11). Atlas Genet Cytogenet Oncol Haematol. 2018;2:51.
21. Joh T, Kagami Y, Yamamoto K, et al. Identification of MLL and chimeric MLL

gene products involved in 11q23 translocation and possible mechanisms of leukemogenesis by MLL truncation. Oncogene. 1996;13(9):1945-1953.
22. Iacovino M, Hernandez C, Xu Z, Bajwa G, Prather M, Kyba M. A conserved role for Hox paralog group 4 in regulation of hematopoietic progenitors. Stem Cells Dev. 2009;18(5):783-792.
23. Stavropoulou V, Kaspar S, Brault L, et al. MLL-AF9 expression in hematopoietic stem cells drives a highly invasive AML expressing EMT-related genes linked to poor outcome. Cancer Cell. 2016;30(1):43-58.
24. Thanasopoulou A, Tzankov A, Schwaller J. Potent co-operation between the NUP98-NSD1 fusion and the FLT3-ITD mutation in acute myeloid leukemia induction. Haematologica. 2014;99(9):1465-1471.
25. Franks TM, McCloskey A, Shokirev MN, Benner C, Rathore A, Hetzer MW. Nup98 recruits the Wdr82-Set1A/COMPASS complex to promoters to regulate H3K4 trimethylation in hematopoietic progenitor cells. Genes Dev. 2017;31(22):2222-2234.
26. Zuber J, Shi J, Wang E, et al. RNAi screen identifies Brd4 as a therapeutic target in acute myeloid leukaemia. Nature. 2011;478(7370):524-528.
27. Stavropoulou V, Almosailleakh M, Royo H, et al. A novel inducible mouse model of MLL-ENL-driven mixed-lineage acute leukemia. HemaSphere. 2018;2(4):e51.
28. Milne TA. Mouse models of MLL leukemia: recapitulating the human disease. Blood. 2017;129(16):2217-2223.
29. Fisher JN, Stavropoulou V, Kalleda N, Schwaller J. The impact of the cellular origin in acute myeloid leukemia: learning from mouse models. Hemasphere. 2019;3(1):e152.
30. Lin YW, Slape C, Zhang Z, Aplan PD. NUP98-HOXD13 transgenic mice develop a highly penetrant, severe myelodysplastic syndrome that progresses to acute leukemia. Blood. 2005;106(1):287-295.
31. Slape C, Liu LY, Beachy S, Aplan PD. Leukemic transformation in mice expressing a NUP98-HOXD13 transgene is accompanied by spontaneous mutations in Nras, Kras, and Cbl. Blood. 2008;112(5):2017-2019.
32. Pineault N, Buske C, Feuring-Buske M, et al. Induction of acute myeloid leukemia in mice by the human leukemia-specific fusion gene NUP98-HOXD13 in concert with Meis1. Blood. 2003;101(11):4529-4538.
33. Slape C, Hartung H, Lin YW, Bies J, Wolff L, Aplan PD. Retroviral insertional mutagenesis identifies genes that collaborate with NUP98-HOXD13 during leukemic transformation. Cancer Res. 2007;67(11):5148-5155.
34. Humeniuk R, Koller R, Bies J, Aplan P, Wolff L. Brief report: loss of p15Ink4b accelerates development of myeloid neoplasms in Nup98-HoxD13 transgenic mice. Stem Cells. 2014;32(5):1361-1366.
35. Imren S, Heuser M, Gasparetto M, et al. Modeling de novo leukemogenesis from human cord blood with MN1 and NUP98HOXD13. Blood. 2014;124(24):3608-3612.
36. Greenblatt S, Li L, Slape C, et al. Knock-in of a FLT3/ITD mutation cooperates with a NUP98-HOXD13 fusion to generate acute myeloid leukemia in a mouse model. Blood. 2012;119(12):2883-2894.
37. Liu H, Cheng EH, Hsieh JJ. Bimodal degradation of MLL by SCFSkp2 and APCCdc20 assures cell cycle execution: a critical regulatory circuit lost in leukemogenic MLL fusions. Genes Dev. 2007;21(19):2385-2398.
38. Liu H, Takeda S, Kumar R, et al. Phosphorylation of MLL by ATR is required for execution of mammalian S-phase checkpoint. Nature. 2010;467(7313):343-346.
39. Chua KF, Mostoslavsky R, Lombard DB, et al. Mammalian SIRT1 limits replicative life span in response to chronic genotoxic stress. Cell Metab. 2005;2(1):67-76.
40. Brunet A, Sweeney LB, Sturgill JF, et al. Stress-dependent regulation of FOXO transcription factors by the SIRT1 deacetylase. Science. 2004;303(5666):2011-2015.
41. Tran D, Bergholz J, Zhang H, et al. Insulin-like growth factor-1 regulates the SIRT1-p53 pathway in cellular senescence. Aging Cell. 2014;13(4):669-678.
42. Duan L, Maki CG. The IGF-1R/AKT pathway determines cell fate in response to p53. Transl Cancer Res. 2016;5(6):664-675.
43. Park AM, Tsunoda I, Yoshie O. Heat shock protein 27 promotes cell cycle progression by down-regulating E2F transcription factor 4 and retinoblastoma family protein p130. J Biol Chem. 2018;293(41):15815-15826.
44. Kim NW, Piatyszek MA, Prowse KR, et al. Specific association of human telomerase activity with immortal cells and cancer. Science. 1994;266(5193):2011-2015.
45. Cesare AJ, Reddel RR. Alternative lengthening of telomeres: models, mechanisms and implications. Nat Rev Genet. 2010;11(5):319-330.
46. Katakura Y, Udono M, Katsuki K, et al. Protein kinase C delta plays a key role in cellular senescence programs of human normal diploid cells. J Biochem. 2009;146(1):87-93.
47. Shi A, Murai MJ, He S, et al. Structural insights into inhibition of the bivalent menin-MLL interaction by small molecules in leukemia. Blood. 2012;120(23):4461-4469.
48. Filippakopoulos P, Qi J, Picaud S, et al. Selective inhibition of BET bromodomains. Nature. 2010;468(7327):1067-1073.